Nanoscale

Accepted Manuscript

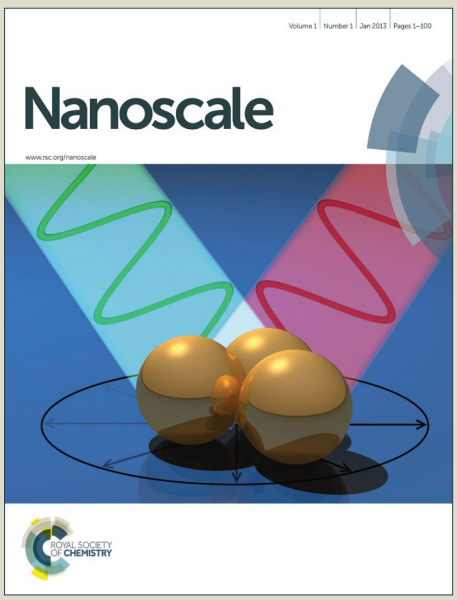

ROYAL SOCIETY OF CHEMISTRY

www.rsc.org/nanoscale

Journal Name

COMMUNICATION

Host-Guest Interaction Induced Supramolecular Amphiphilic Star Architecture and Uniform Nanovesicle Formation for Anticancer Drug Delivery

Received 00th January 20xx,
Accepted 00th January 20xx

DOI: 10.1039/x0xx00000x

www.rsc.org/

Jing-ling Zhu,[a] Kerh Li Liu,[b] Yuting Wen,[a] Xia Song[a] and Jun Li*[a,b]

A star polymer of poly[(R,S)-3-hydroxybutyrate] (PHB) with adamantyl end-terminals extended from an α-cyclodextrin (α-CD) core is designed. It subsequently self-assembles to form controllable and uniform nanovesicles induced by host-guest interaction between heptakis(2,6-di-O-methyl)-β-CD and the adamantyl ends. The nanovesicles are suitable for loading and intracellular delivery of anticancer drug doxorubicin.

Self-assembly of block copolymers has attracted sustained attention due to their immense potential applications,[1-3] especially for biomedical purposes such as drug and gene delivery.[4-8] In the past decades, numerous self-assembled nanostructures, including micelles, vesicles and spheres have been developed.[9-12] The diversity of polymer chemistry provides possibilities to tune the morphology of these self-assembled structures with a "bottom up" approach.[13-15] The morphology and property of the self-assembled nanostructures are primarily determined by the polymer architecture and chemical composition.[16-19] Micelles and vesicles self-assembled from linear block copolymers are the most widely studied nanostructures, although nanostructures constructed from nonlinear block copolymers, with star shaped,[20-23] linear-dendritic,[24-26] or comb shaped[18] architectures, have also been reported.

Novel polymer architecture of nonlinear block copolymer may potentially lead to self-assembled morphology and property not accessible by a linear counterpart.[27-29] In a previous work, we reported an amphiphilic star-block copolymer comprising a star-shaped poly(ethylene glycol) (PEG) core extended with adamantyl (Ada)-terminated poly[(*R,S*)-3-hydroxybutyrate)] (PHB), which shows self-assembly behavior leading to formation of nanogel-like large compound micelles (LCMs) and cyclodextrin (CD)-induced vesicles.[30] However, the highly hydrophilic PEG core caused complexity in controlling the morphology of the self-assembly in aqueous environment, leading to formation of mixed morpholog

In this work, we have designed a star polymer architecture based on a compact α-CD core with multiple PHB arms and Ada terminals (CD-s-PHB-Ada) (Scheme 1a), which was interestingly

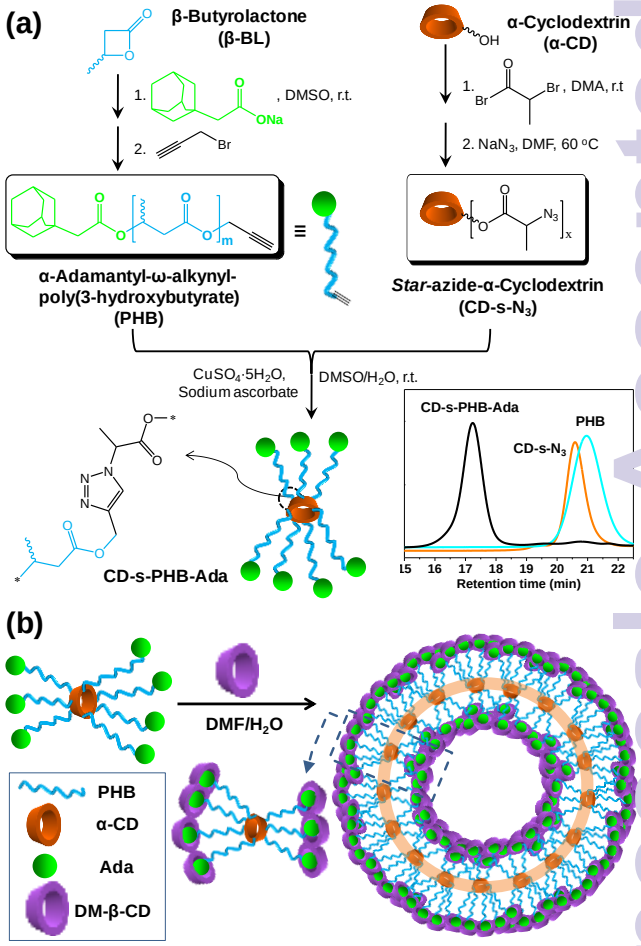

Scheme 1. (a) Synthetic route of PHB based star polymer (CD-s-PHB-Ada) with peripheral adamantyl moiety. On the lower right corner are GPC traces of CD-s-PHB-Ada and its precursors; (b) Schematic representation on the formation of DM-β-CD/CD-s-PHB-Ada nanovesicles.

[a] *Department of Biomedical Engineering, Faculty of Engineering, National University of Singapore, 7 Engineering Drive 1, Singapore 117574, Singapore. Fax: (+65)6872-3069 E-mail: jun-li@nus.edu.sg*
[b] *Institute of Materials Research and Engineering, A*STAR (Agency for Science, Technology and Research), 2 Fusionopolis Way, Singapore 138634, Singapore*
Electronic Supplementary Information (ESI) available: [Polymer synthesis, characterization, preparation of drug-loaded nanovesicles, intracellular drug release and cytotoxicity assays, TEM and DLS measurements]. See DOI: 10.1039/x0xx00000x

found to form controllable and uniform nanovesicles induced by the supramolecular host-guest complexation between heptakis(2,6-di-O-methyl)-β-cyclodextrin (DM-β-CD) (Scheme S1 in Supporting Information) and the Ada ends, transforming the hydrophobic Ada to very hydrophilic and bulky end caps (the DM-β-CD/Ada complexes) (Scheme 1b). The nanovesicles not only mimic liposome self-assembly, but also are superior to liposomes due to the highly hydrophobic PHB arms restricted by the α-CD core which form a thick, stable, and less permeable vesicle wall. In addition, with the biodegradable PHB and the suitable nanoscale size, the nanovesicles are hypothesized to be robust for drug loading and intracellular delivery. To prove the hypothesis, the nanovesicles were employed to load anticancer drug doxorubicin (DOX), and the intracellular drug delivery and cellular toxicity were investigated. It is also interesting that cyclodextrin serves dual roles in the system: α-CD as a structural unit for the star architecture, and β-CD as a host to induce the nanovesicle self-assembly, and both are critical factors leading to such self-assembly behaviors.

The star polymer consisting of α-CD core and PHB arms (CD-s-PHB-Ada) was synthesized through alkyne-azide coupling reaction between heterofunctionalized PHB and azide-functionalized α-CD (CD-s-N_3), as shown in Scheme 1a. Heterofunctionalized PHB, with telechelic adamantyl moiety and alkynyl functionality, was synthesized in a one pot fashion by anionic ring opening polymerization (ROP) of racemic β-butyrolactone, according to the procedure we reported earlier.[30] The degree of polymerization (DP) and M_n of PHB were evaluated to be 9 and 1.01 kD, respectively, based on the intensity ratio of PHB methine proton at around δ 5.2 ppm to alkynyl end group protons at around δ 4.7 ppm in the ^{1}H NMR spectrum (see Figure S1 in Supporting Information). CD-s-N_3 was synthesized by substitution reaction. The number of azide groups in each CD molecule was estimated to be around 13 by ^{1}H NMR and elemental analyses (EA) measurements. The molecular weight of CD-s-N_3 was evaluated to be 2.23 kDa. The successful syntheses of all the macromolecules were first demonstrated by ^{13}C NMR as shown in Figure S2 (Supporting Information).

The successful synthesis of the CD-s-PHB-Ada star polymers was further evidenced by gel permeation chromatography (GPC) analyses. As shown in Scheme 1a, the size of CD-s-PHB-Ada shifted to higher molecular weight region as compared to its two precursors. GPC measurement gave a narrow molecular weight distribution (PDI=1.07) for the star polymer, indicating an efficient and uniform PHB conjugation onto the α-CD core. The chemical structure of the CD-s-PHB-Ada copolymer was elucidated by ^{1}H NMR spectroscopy (Figure S3, Supporting Information). All signals in the spectrum can be ascribed to protons belonging to either PHB, α-CD, linkage segment or adamantyl end group. In particular, the appearance of triazole proton signal at δ 7.8~8.0 ppm attested to the successful alkyne-azide coupling reaction. In addition, the decrease of azide functionality after coupling reaction as evidenced by FTIR in Figure S4 (Supporting Information) further indicates the successful PHB conjugation onto α-CD core. The M_n and arm number of the star polymer were estimated to be 9.28 kDa and 7.0, respectively, by ^{1}H NMR and EA measurements.

Due to the high hydrophobicity of PHB, CD-s-PHB-Ada with a high fraction of PHB cannot be dissolved in water directly. To prepare micellar solutions, CD-s-PHB-Ada was first dissolved in DMF, then diluted with water to induce self-assembly. As CD-s-PHB-Ada is terminated by adamantane (Ada), β-CD derivatives are supposed to modulate the self-assembly behavior of CD-s-PHB-Ada in aqueous solution via host-guest interaction.[31-33] Here we choose the highly hydrophilic DM-β-CD which has a donut-shaped molecular structure with a hydrophobic cavity that binds strongly to Ada. A series of DM-β-CD/CD-s-PHB-Ada micellar solutions at various weight ratios were prepared by adding 900 μL of water to 100 μL of CD-s-PHB-Ada and DM-β-CD in DMF. The CD-s-PHB-Ada concentration was fixed and the volume ratio of DMF is 10 % in the final aqueous solution.

The particle size of freshly prepared DM-β-CD/CD-s-PHB-Ada micellar solutions were determined by using dynamic light scattering (DLS). The hydrodynamic radii (R_h) (z-average) of DM-β-CD/CD-s-PHB-Ada micellar solutions as a function of composition (weight ratio of DM-β-CD to CD-s-PHB-Ada) are plotted and shown in Figure 1(a). Firstly, the CD-s-PHB-Ada star polymers were found to self-assemble into particles with R_h at around 60 nm in the absence of DM-β-CD. The particle size increased abruptly when a small quantity of DM-β-CD was added, giving large R_h values at the DM-β-CD/CD-s-PHB-Ada weight ratio from 1 – 5. The particles formed within this ratio range precipitated quickly. The R_h became smaller and stable when the DM-β-CD/CD-s-PHB-Ada weight ratio reached 7.5 or higher. It is noted that CD-s-PHB-Ada with relatively high hydrophobicity can form nanoparticles which may be stabilized by the hydrophilic CD part. The addition of DM-β-CD should have broken the previous hydrophilic-hydrophobic balance and induced re-self-assembly. The morphologies of the aggregates at different DM-β-CD/CD-s-PHB-Ada weight ratio were observed by transmission electron microscopy (TEM), as shown in Figure 1(b). The colloidal solution of CD-s-PHB-Ada (ratio 0) was found to form solid particles. The morphologies of DM-β-CD/CD-s-PHB-Ada aggregates at ratios 7.5 and 15 were found to be irregular hollow structures, while more regular and spherical vesicles formed at ratio 20 or higher.

The AFM image further confirmed the vesicular structure of the DM-β-CD/CD-s-PHB-Ada (20:1) aggregates (Figure 2). The cross section profile of AFM image showed that the height decreased from the outer edges to the center of the particles, indicating the hollow nature of the vesicles (Figure 2b). The AFM results showed good agreement with the TEM images of the DM-β-CD/CD-s-PHB-Ada nanovesicles (Figure 2c). Considering both the restrictive nature of the star architecture and the hydrophobic properties of PHB, we propose a possible model for the supramolecular self-assembly of DM-β-CD/CD-s-PHB-Ada (20:1), as illustrated in

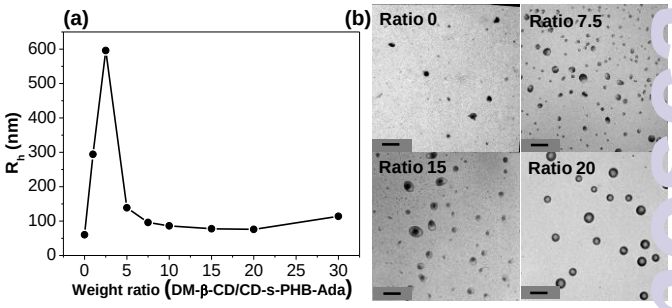

Figure 1. (a) R_h (z-average) of DM-β-CD/CD-s-PHB-Ada micellar solutions as a function of composition (weight ratio of DM-β-CD to CD-s-PHB-Ada). All the samples were measured after freshly prepared. (b) TEM images of DM-β-CD/CD-s-PHB-Ada complexes at various weight ratios. The scale bars represent 500 nm.

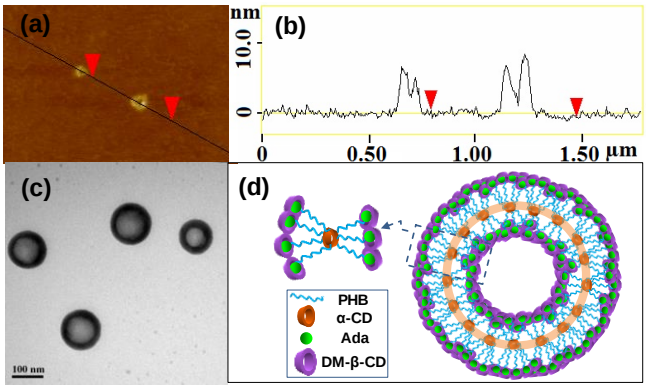

Figure 2. (a) AFM image of DM-β-CD/CD-s-PHB-Ada (20:1) aggregates and (b) the corresponding cross-section profile; (c) TEM image of DM-β-CD/CD-s-PHB-Ada (20:1) aggregates; (d) Schematic representation on the self-assembly of DM-β-CD/CD-s-PHB-Ada nanovesicles.

Figure 2(d). The vesicle wall was formed by PHB aggregation with the embedded α-CD core while its exterior and interior surfaces were covered with hydrophilic DM-β-CD through forming stable inclusion complex with the Ada moiety. The vesicles formed by DM-β-CD/CD-s-PHB-Ada (20:1) had a size of around 100 nm, which is favorable for their application as drug carrier systems. In order to observe the influence of preparation methods on the vesicle formation, we prepared DM-β-CD/CD-s-PHB-Ada (20:1) self-assemblies by three other methods to compare with the above used method. The three methods are (a) simply injecting DMF solution of DM-β-CD/CD-s-PHB-Ada (20:1) into an aqueous solution, (b) rehydrating CD-s-PHB-Ada film with DM-β-CD aqueous solution, and (c) adding water (pH=3) to DMF solution of DM-β-CD/fluorescein-labeled CD-s-PHB-Ada (CD-s-PHB-Ada-FITC) (20:1) and dialyzing against water (pH=7) for DOX loading and DMF removal. Compared to the original method used in this study, we changed the sequence of adding DMF and water in method (a). The influence of solvent was excluded in method (b). Method (c) was developed for drug loading and cellular uptake study. DLS and TEM measurements confirmed the formation of nano-sized vesicles by any of these methods, as shown in Figure S7 (Supporting Information).

One of the main strategies to target specific morphology of amphiphiles is to alter the packing parameter (p).[34, 35] In the case of block copolymers, hydrophilic block fraction ($f_{hydrophilic}$) reflecting the packing factor is preferred to be used rather than p.[36, 37] To further understand the self-assembly behavior of the CD-s-PHB-Ada star polymer with DM-β-CD and its morphology, we synthesized a control polymer, CD-s-PHB-MPEG, with methoxy-PEG replacing Ada of CD-s-PHB-Ada (Figure S5, Supporting Information). The chemical structures of CD-s-PHB-MPEG and its precursor PHB-MPEG were elucidated by ^{1}H NMR spectra (Figure S6, Supporting Information). The PHB length and arm number of CD-s-PHB-MPEG were close to those of CD-s-PHB-Ada, and the hydrophilicity of MPEG (1.9 k) was much higher than Ada/DM-β-CD complex, so the hydrophilic fraction ($f_{hydrophilic}$) of CD-s-PHB-MPEG is higher than that of DM-β-CD/CD-s-PHB-Ada. The star polymers with/without DM-β-CD in this study are arranged in order of $f_{hydrophilic}$, as shown in Figure 3.

It is reported that, by adjusting the packing factor of linear diblock copolymers, vesicles are favored when $f_{hydrophilic}$ is around

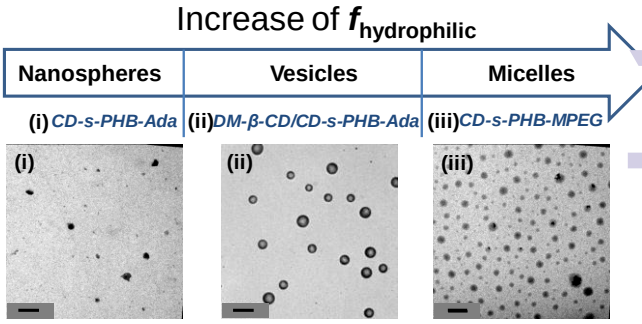

Figure 3. The ordering of $f_{hydrophilic}$ of star polymers in this study and their corresponding self-assembled morphologies. The scale bars represent 500 nm.

35±10 %, while micelle is formed when $f_{hydrophilic}$ > 45%.[37] In th study, DM-β-CD/CD-s-PHB-Ada (20:1) that had moderate $f_{hydrophilic}$ was found to form vesicles. The CD-s-PHB-MPEG that had highest $f_{hydrophilic}$ should form conventional core-shell micelles, while CD-s-PHB-Ada with very high hydrophobicity should f nanospheres. The TEM images in Figure 3 provide evidence that specific morphologies could be targeted by adjusting $f_{hydrophilic}$ of star polymer architectures.

The DM-β-CD/CD-s-PHB-Ada (20:1) nanovesicles were used to load the anticancer drug, doxorubicin hydrochloride (DOX), t evaluate their potential for drug delivery application. DOX is a fluorescent compound that can be easily traced in the process o intracellular uptake. Here CD-s-PHB-Ada was also labeled b fluorescein. A pH-gradient method[38] was used to facilitat encapsulation of DOX into the nanovesicles. The drug loadin efficiency and loading content were estimated to be 38.8% an 0.31%, respectively, at drug/nanovesicles feed ratio of 0.8/10 (wt/wt). As indicated in Figure S7(c), DM-β-CD/CD-s-PHB-Ada-FIT (20:1) kept the vesicular structure even after drug loading an organic solvent removal.

Hela cells were cultured with the DOX-loaded FITC-labeled nanovesicles over different periods of time. In Figure 4(a), ti dependent confocal microscopic images were used to investigate the intracellular uptake of the DOX-loaded nanovesicles and the delivery of DOX from the nanovesicles. Free DOX with equivalen concentrations were used as comprison (Figure 4b). The location o DOX can be tracked from the red fluorescence, and the informa about nanovesicles can be obtained from the green fluorescence i the FITC channel. At the beginning (1 h), DOX was internalized int Hela cells with the nanovesicles, and the red fluorescence appeare where the nanovesicles were. After 2 h incubation, the increasin number of nanovesicles and DOX appeared inside the cells. It is noted that the red fluorescence was localized together with th green fluorescence in the cytoplasm at the early stages (1 and 2 h) only weak red fluorescence was observed in the nucleus at 2 After 4 h incubation, both cytoplasm and nucleus were dyed red, while green fluorescence was only seen in the cytoplasm, indicatin that the nanovesicles could not enter the nucleus. The red fluorescence in the nucleus was attributed to the release of DO from the nanovesicles. Then after 8 h incubation, most red fluorescence was found to locate in the nucleus, indicating most DOX was released from the nanovesicles and entered the

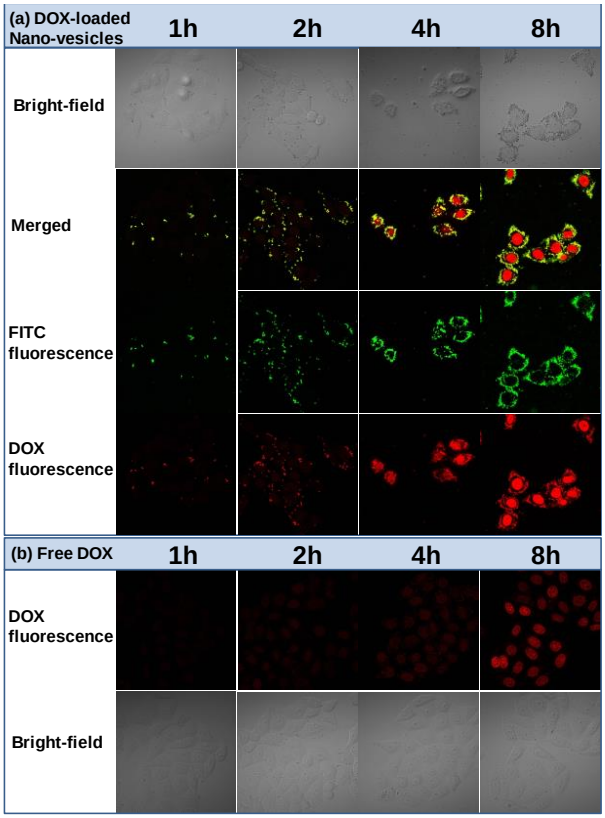

Figure 4. Confocal microscopy images of Hela cells treated with (a) DOX-loaded nanovesicles and (b) free DOX with equivalent DOX concentration (4 μg/mL) for 1, 2, 4, and 8 h.

nucleus. The gradual release of DOX from the nanostructures intracellularly was also reported by other researchers.[39, 40] In contrast, free DOX was taken by the cells and delivered to the nucleus in a much less efficient manner (Figure 4b).

The cytotoxicity effect of DOX-loaded nanovesicles was studied *in vitro* with Hela cells using the MTT assay. For comparison, the cytotoxicity of free DOX and blank nanovesicles was also evaluated. The blank nanovesicles were prepared through the same process as that for the DOX-loaded nanovesicles except for adding DOX, and the nanovesicles concentration was adjusted to be the same after dialysis. The serial blank nanovesicles without DOX were prepared by stepwise dilution from blank nanovesicles with the same initial concentration as that of DOX-loaded nanovesicles. From Figure 5, it was found that the cytotoxicity of DOX-loaded nanovesicles was higher than that of the free DOX, while the blank nanovesicles showed no cytotoxicity within the tested concentrations. The reason that the nanovesicles enhanced the cytotoxicity may be attributed to the efficient intracellular uptake of the DOX-loaded nanovesicles, by an endocytosis mechanism,[41, 42] compared to a passive diffusion mechanism involved in the free DOX delivery.

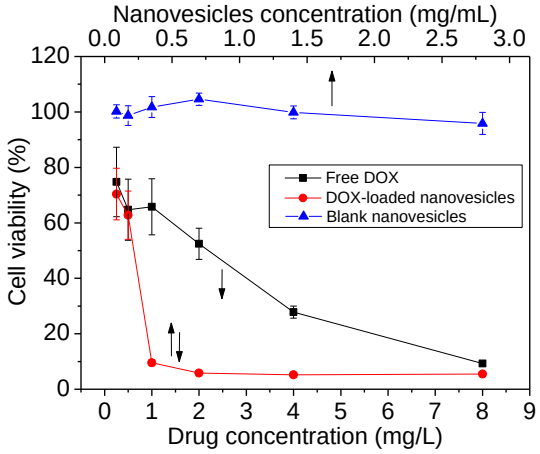

Figure 5. Cytotoxicity of DOX-loaded nanovesicles (♦), free DOX with equivalent concentrations (■) and blank nanovesicles (▲) on Hela cells. The serial blank nanovesicles without DOX were prepared by stepwise dilution from blank nanovesicles with the same initial concentration as that of DOX-loaded nanovesicles.

Conclusions

In summary, we have constructed a star polymer of PHB with Ada end-terminals extended from α-CD core, which formed inclusion complexes with DM-β-CD to give a supramolecular amphiphilic star architecture comprising multiple highly hydrophobic PHB arms restricted by the α-CD core and hydrophilic and bulky end caps (the DM-β-CD/Ada complexes). The supramolecular amphiphilic star architecture subsequently self-assembled to form controllable and uniform nanovesicles which were found to be suitable for loading and intracellular delivery of anticancer drug DOX. Through efficient intracellular uptake, the DOX-loaded nanovesicles were much more powerful in killing cancer cells compared to free DOX. It is also interesting that cyclodextrin serves dual roles in the system: α-CD as a structural unit for the star architecture, and β-CD as a host to induce the nanovesicle self-assembly. We believe that the host-guest interaction directed nano-morphology control and nanovesicle formation demonstrated here encompasses a robust and modular strategy that could be adopted for design of self-assembly systems and construction of other useful nanostructures.

Acknowledgements

We acknowledge the support from Ministry of Education Singapore (Grant No. R-397-000-188-112 and R-397-000-136-112), National University of Singapore (Grant No. R-397-000-136-731), and Agency for Science, Technology and Research (A*STAR), Singapore (Grant No. 132 148 0007).

Notes and references

1 Z. Ge and S. Liu, *Chem. Soc. Rev.*, 2013, **42**, 7289-7325.

2 Y. Gu, J. G. Werner, R. M. Dorin, S. W. Robbins and U. Wiesner, *Nanoscale*, 2015, **7**, 5826-5834.
3 M. Stefik, S. Guldin, S. Vignolini, U. Wiesner and U. Steiner, *Chem. Soc. Rev.*, 2015.
4 K. Cai, X. He, Z. Song, Q. Yin, Y. Zhang, F. M. Uckun, C. Jiang and J. Cheng, *J. Am. Chem. Soc.*, 2015, **137**, 3458-3461.
5 Z.-X. Zhao, S.-Y. Gao, J.-C. Wang, C.-J. Chen, E.-Y. Zhao, W.-J. Hou, Q. Feng, L.-Y. Gao, X.-Y. Liu, L.-R. Zhang and Q. Zhang, *Biomaterials*, 2012, **33**, 6793-6807.
6 C. Y. Zhang, Y. Q. Yang, T. X. Huang, B. Zhao, X. D. Guo, J. F. Wang and L. J. Zhang, *Biomaterials*, 2012, **33**, 6273-6283.
7 Q. Zhang, N. Re Ko and J. Kwon Oh, *Chem. Commun.*, 2012, **48**, 7542-7552.
8 S. Bi, Y. Dong, X. Jia, M. Chen, H. Zhong and B. Ji, *Nanoscale*, 2015, **7**, 7361-7367.
9 W. M. Park and J. A. Champion, *J. Am. Chem. Soc.*, 2014, **136**, 17906-17909.
10 C. Wang, Z. Wang and X. Zhang, *Acc. Chem. Res.*, 2012, **45**, 608-618.
11 P. Tanner, P. Baumann, R. Enea, O. Onaca, C. Palivan and W. Meier, *Acc. Chem. Res.*, 2011, **44**, 1039-1049.
12 T. Smart, H. Lomas, M. Massignani, M. V. Flores-Merino, L. R. Perez and G. Battaglia, *Nano Today*, 2008, **3**, 38-46.
13 Y. Zhang, H. F. Chan and K. W. Leong, *Adv. Drug Del. Rev.*, 2013, **65**, 104-120.
14 N. Hadjichristidis, S. Pispas and G. Floudas, in *Block Copolymers*, John Wiley & Sons, Inc., 2003, pp. 91-113.
15 L. Cademartiri and K. J. M. Bishop, *Nat. Mater.*, 2015, **14**, 2-9.
16 Y. Sanada, I. Akiba, S. Hashida, K. Sakurai, K. Shiraishi, M. Yokoyama, N. Yagi, Y. Shinohara and Y. Amemiya, *J. Phys. Chem. B*, 2012, **116**, 8241-8250.
17 P. J. M. Stals, Y. Li, J. Burdyńska, R. Nicolaÿ, A. Nese, A. R. A. Palmans, E. W. Meijer, K. Matyjaszewski and S. S. Sheiko, *J. Am. Chem. Soc.*, 2013, **135**, 11421-11424.
18 W. S. Chiang, C. H. Lin, B. Nandan, C. L. Yeh, M. H. Rahman, W. C. Chen and H. L. Chen, *Macromolecules*, 2008, **41**, 8138-8147.
19 A. Kalogirou, O. A. Moultos, L. N. Gergidis and C. Vlahos, *Macromolecules*, 2014, **47**, 5851-5859.
20 D. E. Poree, M. D. Giles, L. B. Lawson, J. He and S. M. Grayson, *Biomacromolecules*, 2011, **12**, 898-906.
21 Z. X. Zhang, K. L. Liu and J. Li, *Angew. Chem., Int. Ed.*, 2013, **52**, 6180-6184.
22 Z. X. Zhang, K. L. Liu and J. Li, *Macromolecules*, 2011, **44**, 1182-1193.
23 Z. X. Zhang, X. Liu, F. J. Xu, X. J. Loh, E. T. Kang, K. G. Neoh and J. Li, *Macromolecules*, 2008, **41**, 5967-5970.
24 J. s. del Barrio, L. Oriol, C. Sánchez, J. L. Serrano, A. l. Di Cicco, P. Keller and M.-H. Li, *J. Am. Chem. Soc.*, 2010, **132**, 3762-3769.
25 M. G. Jeong, J. C. M. van Hest and K. T. Kim, *Chem. Commun.*, 2012, **48**, 3590-3592.
26 A. Sousa-Herves, C. Sanchez Espinel, A. Fahmi, A. Gonzalez-Fernandez and E. Fernandez-Megia, *Nanoscale*, 2015, **7**, 3933-3940.
27 Y. Wang and S. M. Grayson, *Adv. Drug Del. Rev.*, 2012, **64**, 852-865.
28 J. Xu, Z. S. Ge, Z. Y. Zhu, S. Z. Luo, H. W. Liu and S. Y. Liu, *Macromolecules*, 2006, **39**, 8178-8185.
29 Z. S. Ge and S. Y. Liu, *Macromol. Rapid Commun.*, 2009, **30**, 1523-1532.
30 J.-L. Zhu, K. L. Liu, Z. Zhang, X.-Z. Zhang and J. Li, *Chem. Commun.*, 2011, **47**, 12849-12851.
31 A. Sandier, W. Brown, H. Mays and C. Amiel, *Langmuir*, 2000, **16**, 1634-1642.
32 J. Carrazana, A. Jover, F. Meijide, V. H. Soto and J. V. Tato, *J Phys Chem B*, 2005, **109**, 9719-9726.
33 D. Harries, D. C. Rau and V. A. Parsegian, *J Am Chem Soc*, 2005, **127**, 2184-2190.
34 J. N. Israelachvili, in *Intermolecular and Surface Forces (Third Edition)*, Academic Press, San Diego, 2011, pp. 535-576.
35 R. Nagarajan, in *Amphiphiles: Molecular Assembly and Applications*, American Chemical Society, 2011, vol. 1070, ch. 1, pp. 1-22.
36 D. E. Discher, V. Ortiz, G. Srinivas, M. L. Klein, Y. Kim, D. Christian, S. Cai, P. Photos and F. Ahmed, *Prog Polym Sci*, 2007, **32**, 838-857.
37 D. E. Discher and A. Eisenberg, *Science*, 2002, **297**, 967-973.
38 L. Mayer, M. Bally and P. Cullis, *Biochimica et Biophysica Acta (BBA)-Biomembranes*, 1986, **857**, 123-126.
39 M. Oishi, H. Hayashi, M. Iijima and Y. Nagasaki, *J Mater Chem*, 2007, **17**, 3720-3725.
40 B. Kang, J. Li, S. Chang, M. Dai, C. Ren, Y. Dai and D. Chen, *Small*, 2012, **8**, 777-782.
41 C. Muhlfeld, P. Gehr and B. Rothen-Rutishauser, *Swiss Med Wkly*, 2008, **138**, 387-391.
42 T.-G. Iversen, T. Skotland and K. Sandvig, *Nano Today*, 2011, **6**, 176-185.